Structural Transition of Friedel's Salt 3CaO·Al2O3·CaCl2·10H2O Studied by Synchrotron Powder Diffraction

4 AUTHORS, INCLUDING:

Guillaume Renaudin
Ecole Nationale Supérieure de Chimie de Cl…
92 PUBLICATIONS **1,824** CITATIONS

SEE PROFILE

Michel François
University of Lorraine
124 PUBLICATIONS **2,205** CITATIONS

SEE PROFILE

Structural transition of Friedel's salt $3CaO \cdot Al_2O_3 \cdot CaCl_2 \cdot 10H_2O$ studied by synchrotron powder diffraction

J.-P. Rapin[a], G. Renaudin[b], E. Elkaim[c], M. Francois[a],*

[a]*Laboratoire de Chimie du Solide Minéral-UMR 7555, Université Henri Poincaré, Nancy I-F-54506 Vandoeuvre les Nancy, B.P. 239 Nancy, France*
[b]*Laboratoire de Cristallographie, Université de Genève, 24 quai Ernest Ansermet CH-1211 Genève 4, Switzerland*
[c]*Laboratoire LURE, Bat 209D, Centre Universitaire Paris Sud, BP 34, 91898 Orsay Cedex, France*

Abstract

The structural phase transition occurring in Friedel's salt, the chlorinated compound $3CaO \cdot Al_2O_3 \cdot CaCl_2 \cdot 10H_2O$ (AFm phase), was studied by synchrotron and standard X-ray powder diffraction. The compound transforms at 35 °C from a rhombohedral (rh) high-temperature (HT) phase [$R - 3c$; $a = 5.744(2)$ Å, $c = 46.890(3)$ Å] to a monoclinic (m) low-temperature (LT) phase [$C2/c$; $a = 9.960(4)$ Å, $b = 5.7320(2)$ Å, $c = 16.268(7)$ Å, $\beta = 104.471(2)°$]. The LT and HT phases were refined with the Rietveld method from synchrotron data recorded at 20 and 40 °C. Variations of the lattice parameters as a function of temperature are reported between 8 and 48 °C. The rh → m transition is characterized by a unit cell volume expansion of 1% and a movement of the interlayer species: a shift of 0.45 Å of the Cl^- anions along $[010]_h$ and a shift of 0.25 Å of the water molecules along $[210]_h$ of the hexagonal cell. The m phase distortion is due to an ordering of the hydrogen bonds between chloride anions and H-atoms of the water molecules. © 2002 Elsevier Science Ltd. All rights reserved.

Keywords: Crystal structure; X-ray diffraction; Synchrotron radiation; Chloride; Friedel's salt; Structural transition

1. Introduction

Friedel's salt is the common name of the chlorinated lamellar double hydroxide (LDH) of composition $3CaO \cdot Al_2O_3 \cdot CaCl_2 \cdot 10H_2O$. This compound was for the first time mentioned by Friedel [1] in 1897, who studied the reactivity of lime with aluminum chloride. The hydrated tetracalcium bichloroaluminate belongs to AFm phases and is part of a family of hydrated compounds found in cement pastes. The AFm phases are composed of positively charged main layers $[Ca_2Al(OH)_6]^+$ and negatively charged interlayers $[X^-, nH_2O]$ where X^- is a mineral anion. AFm phases for which the structures were solved from single crystal data contain the following anions: Cl^- [2,3], Br^- [4], I^- [5], SO_4^{2-} [6], CO_3^{2-} [7,8] and NO_3^- [9]. The O-coordination numbers of the Al^{3+} and Ca^{2+} ions in these phases are 6 and 7, respectively. Each Ca^{2+} is approached by a seventh O-atom

of a water molecule or by an O-atom of an oxo-anion. The interlayer of Friedel's salt has the composition $[2H_2O, Cl^-]$. The chloride anions have 10 H-atoms as first neighbors (Cl^- is connected to the structure by H-bonds ClH) and 12 O-atoms as second neighbors (six from hydroxyl groups and six from water molecules).

Friedel's salt presents a structural transition at 35 °C, which was observed by polarized light optical microscopy [2]. We must consider two phases for this compound: the low-temperature (LT) form and the high-temperature (HT) modification. The LT form [monoclinic (m) space group $C2/c$] was solved by single crystal X-ray diffraction at room temperature by Terzis et al. [3], but the given atomic coordinates are partly erroneous. Our attempts to use the coordinates of the LT form reported by Terzis to refine our powder spectra by the Rietveld method were unsuccessful. The HT structure [rhombohedral (rh) space group $R - 3c$] was determined later by single crystal X-ray diffraction at 40 °C [2].

We chose to study the title compound by X-ray powder diffraction as a function of temperature to determine the changes occurring during the transition. For this purpose, we used synchrotron radiation in order to obtain

* Corresponding author. Tel.: +33-3-83-91-24-99; fax: +33-3-83-91-21-66.
E-mail address: michel.francois@lcsm.uhp-nancy.fr (M. Francois).

Table 1
Experimental parameters for synchrotron radiation experiment

	Wavelength (Å)	2θ range (°)	Counting time (h)	Step (°)
$T = 20$ °C	0.82111	1–75	3.1	0.010
$T = 40$ °C	1.06920	4–86	2.8	0.012

data of quality allowing the refinement of structural models by the Rietveld method. Our intention was also to reexamine the LT phase by using the direct methods for solving the crystallographic structures.

Supplementary X-ray analyses as a function of temperature were carried out to determine the lattice parameter variations. The transition is also observed by differential scanning calorimetry (DSC).

2. Experimental

2.1. Sample preparation and thermal analysis

Crystalline samples with composition of $3CaO \cdot Al_2O_3 \cdot CaCl_2 \cdot 10H_2O$ were prepared by hydrothermal synthesis as described in Refs. [7–9]. The starting powder is a homogeneous mixture of $Ca(OH)_2$, $Al(OH)_3$ and $CaCl_2 \cdot 6H_2O$ (Prolabo products) in molar ratios of 3:2:1. The product is put into a INEL CPS 120 diffractometer (INEL, Artenay, France) to verify its purity and crystallinity. The diagram is first analyzed using the DIFFRAC-AT program [10], which includes phase identification using the ICDD Powder Diffraction File Database. The spectrum is completely indexed (no residual phase was detected) with ASTM File 19-0202 reported for Friedel's salt of m phase symmetry. The noncontamination by carbonate on the sample used for further measurement has also been verified by EDS analysis and Raman spectrometry.

DSC over a temperature range from -60 to 500 °C and a heating rate of 5 °C/min under a flowing argon atmosphere was used essentially to detect the phase transition and to determine the transformation energy.

2.2. X-ray diffraction experiments

The title compound was studied by synchrotron radiation using the WDIF4C powder diffractometer on the DW22 beamline of LURE [11]. For this instrument, a monochromatic beam is extracted from the white beam by means of a double Si(111) monochromator. An air blower [12] was employed to heat the sample and control its temperature. The sample was ground to a fine powder (grain size = 1–10 μm) and introduced in a Lindeman tube ($\Phi = 0.5$ mm). Rotation of the sample around the capillary axis was applied to reduce preferred orientation

problems inherent to such layered compounds. Data were recorded at 20 and 40 °C in Debye–Scherrer mode following the experimental parameters reported in Table 1. The averaged width at mid-height (HWMH) of Bragg reflections taken on the whole pattern at 20 or 40 °C is about 0.17° (2θ), so relatively wide compared to those obtained for silicon used as a standard (0.05°). However, this fact is not unusual for such materials and is attributed to a turbostratic disorder. A series of spectra was recorded in the temperature range between 8 and 48 °C at intervals of about 2 °C for 3 h for each temperature in the range 16.0–48.0° (2θ) in steps of 0.02° (2θ) by using an X-Pert Pro diffractometer (Philips, Almelo, The Netherlands), with a Bragg–Brentano geometry, a Ni-filtered Cu$K\alpha$ radiation, a backside monochromator and a TTK 450 HT chamber (Anton Paar, Graz, Austria).

2.3. Diffraction data analysis

The observed LT synchrotron diagram recorded at 20 °C is completely indexed in the m cell with lattice parameters, $a = 9.949$ Å, $b = 5.731$ Å, $c = 16.270$ Å, $\beta = 104.46°$ and space group C2/c, in agreement but slightly different from those given earlier [3]. So, these parameters and space group C2/c are used as input data for the EXTRA program allowing structural resolution by direct methods [13]. The convolution procedure in the measured 2θ range 2.98–75.0° (2θ) leads to the extraction of 1547 hkl reflections of which 422 are independent, with a satisfactory fit factor R of 4.1%. The starting structure solution, which leads to a R Bragg value of 15.2% given by the program, is compatible with the structural formula $[Ca_2Al(OH)_6]^+ [2H_2O, Cl^-]$, meaning that all atomic sites, except H sites, (Ca, Al, Cl, O_{H1}, O_{H2}, O_{H3} for O-atoms of hydroxyl groups and O_W for O-atom of water molecules) are probably well positioned in the lattice.

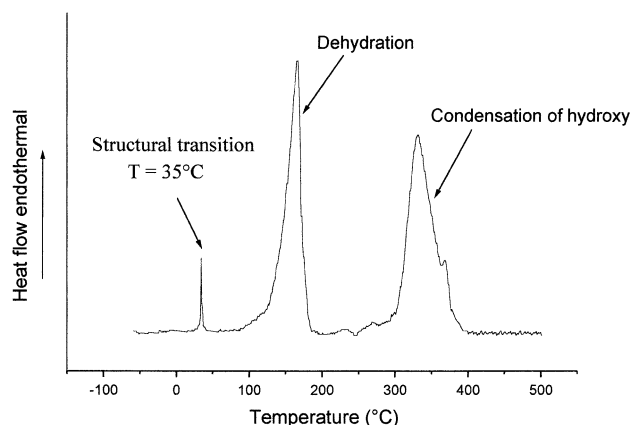Fig. 1. DSC curve of $[Ca_2Al(OH)_6]^+ [2H_2O, Cl^-]$.
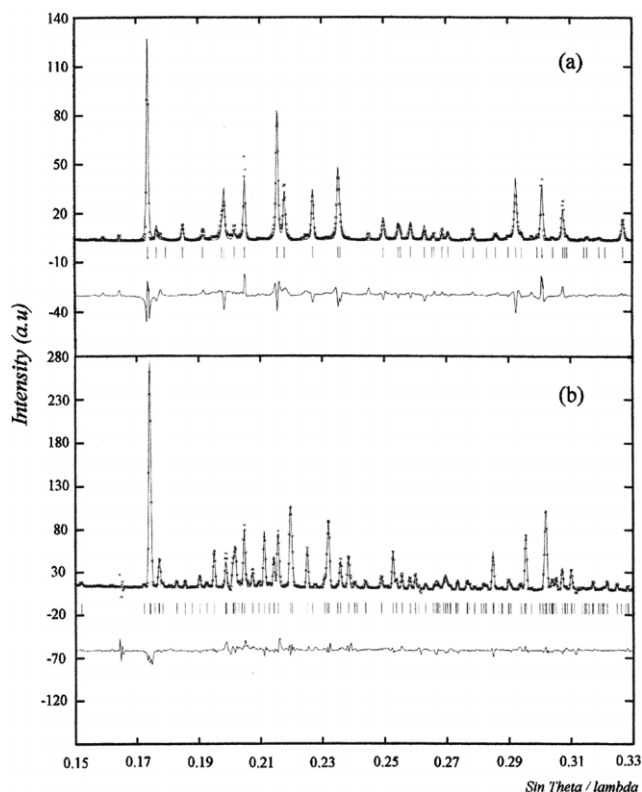
Fig. 2. Selected sin θ/λ ranges of synchrotron diffraction patterns (crosses) of $[Ca_2Al(OH)_6]^+[2H_2O, Cl^-]$ at (a) 40 and (b) 20 °C. Calculated (top) and difference (bottom) patterns.

The HT diagram is completely indexed in the hexagonal lattice ($a = 5.75$ Å, $c = 46.89$ Å, space group R − 3c), meaning that the compound is completely transformed at 40 °C.

Rietveld analyses are performed by using the FULL-PROF program [14]. The starting model for the LT modification is that found by direct methods from synchrotron data. Starting atomic parameters for the HT modification are those reported from single crystal data obtained earlier by the authors [2]. Lattice parameter refinement is performed by using the UFIT program [16].

3. Results and discussion

3.1. DSC results

The DSC curve of the Friedel's salt is represented on Fig. 1. It shows three endothermic peaks: the peak at 35 °C is due to the structural transition, those at 155 and 340 °C correspond to the dehydration (loss of the interlayer water) and the hydroxyl condensation, respectively. As it will be discussed, it is interesting to note that the energy required for the structural transition is 1.5 kcal/mol.

3.2. Rietveld refinement of the LT and HT phases

As can be seen on Fig. 2, the diagram observed at 40 °C differs significantly from that at 20 °C. It can be supposed that important structural changes occur during this first-order phase transition. Results of the structure refinement at 40 and 20 °C are summarized in Tables 2 and 3, respectively, and compared with earlier works. The atomic parameters obtained at 40 °C (rh form) are in agreement with those obtained on a single crystal [2] at the same temperature. They are slightly less accurate but do not differ by more than three standard deviations from the latter.

The atomic coordinates of the m phase obtained at 20 °C are reported in the standard setting (C2/c with origin on glide plane c). For comparing with the Terzis data, which are expressed with the origin on glide plane n, it is necessary to shift these later by 3/4 3/4 0. It appears that

Table 2
Refinement results of $[Ca_2Al(OH)_6]^+[2H_2O, Cl^-]$ at 40 °C

Groups	Atoms	Position	X	Y	Z	B_{iso} [Å^2]	Occupancy
	Al	6 (b)	0	0	0	0.99 (17)	1
			0	**0**	**0**	**1.10 (8)**	1
	Ca	12 (c)	2/3	1/3	0.98758 (7)	0.93 (7)	1
			2/3	**1/3**	**0.9873 (1)**	**1.26 (8)**	**1**
Hydroxyl	O_H	36 (f)	0.0678 (8)	0.3106 (12)	− 0.0213 (1)	1.73 (6)	1
			0.0669 (4)	**0.3071 (4)**	**− 0.0213 (1)**	**1.26 (8)**	**1**
	H		**0.143 (6)**	**0.335 (7)**	**− 0.0391 (4)**	**1.58 (−)**	**1**
Water	O_W	12 (c)	2/3	1/3	0.9345 (2)	a	1
			2/3	**1/3**	**0.9340 (1)**	**4.26 (8)**	**1**
	H_W	36 (f)	**0.57 (2)**	**0.158 (2)**	**0.9261 (7)**	**5.13 (−)**	**2/3**
Chloride	Cl	6 (a)	0	0	1/4	a	1
			0	**0**	**1/4**	**5.29 (8)**	**1**
Atoms	β_{11}		β_{22}	β_{33}	β_{23}	β_{13}	β_{12}
Cl	1068 (49)		1068 (49)	4.5 (0.9)	0	0	42 (25)
O_W	381 (43)		381 (43)	3.8 (1.1)	0	0	− 5 (76)

Number of profile refined parameters: 9. Number of intensity-dependent refined parameters: 15. $R_p = 11.6\%$, $R_{wp} = 16.3\%$, $R_{exp} = 4.3\%$. $R_I = 13.3\%$. Space group R − 3c, $a = 5.755(2)$ Å, $c = 46.97(1)$ Å. In bold, data taken from Renaudin et al. [2].
a Anisotropic temperature factors for interlayer species βij × 10^4.

Table 3
Refinement results of $[Ca_2Al(OH)_6]^+[2H_2O, Cl^-]$ at 20 °C

Groups	Atoms	Position	X	Y	Z	B_{iso} [Å^2]
	Al	4a	3/4	3/4	0	0.79 (15)
			0	**0**	**0**	**0.81**
	Ca	8f	0.0984 (3)	0.7530 (7)	0.0377 (2)	0.76 (6)
			0.34882 (3)	**0.00062 (6)**	**0.03717 (2)**	**1.00**
Hydroxyl	O_{H1}	8f	0.8780 (10)	0.6513 (15)	0.9342 (6)	0.55 (25)
			0.12853 (11)	**0.90438 (21)**	**0.93699 (7)**	**1.12**
	H1		**0.125 (2)**	**0.945 (4)**	**0.893 (2)**	
	O_{H2}	8f	0.8086 (10)	0.4700 (16)	0.0661 (6)	0.12 (21)
			0.52960 (11)	**− 0.27981 (20)**	**0.06193 (7)**	**0.99**
	H2		**0.095 (2)**	**− 0.275 (4)**	**0.105 (2)**	
	O_{H3}	8f	0.5970 (10)	0.5660 (16)	0.9316 (6)	0.49 (22)
			0.84802 (11)	**0.08201 (11)**	**0.93553 (7)**	**1.12**
	H3		**0.845 (2)**	**0.789 (4)**	**0.889 (2)**	
Water	O_W	8f	0.1729 (10)	0.7453 (22)	0.1993 (6)	2.3 (3)
			0.41979 (17)	**0.00443 (27)**	**0.19413 (10)**	**2.69**
	H_{WA}		**0.375 (3)**	**0.896 (5)**	**0.215 (2)**	
	H_{WB}		**0.503 (3)**	**0.999 (5)**	**0.217 (2)**	
Chloride	Cl	4e	0	0.3283 (11)	1/4	2.7 (2)
			1/4	**− 0.42451 (16)**	**1/4**	**2.61**

$R_p = 6.9\%$. Number of profile refined parameters: 11. $R_{wp} = 11.1\%$. Number of intensity-dependent refined parameters: 24. $R_{exp} = 2.7\%$. $R_I = 14.0\%$. Space group C2/c. $a = 9.960(4)$ Å, $b = 5.732(2)$ Å, $c = 16.268(7)$ Å, $\beta = 104.471(2)°$. **$a = 9.979(3)$ Å, $b = 5.751(2)$ Å, $c = 16.320(6)$ Å, $\beta = 104.53(3)°$**. In bold, data taken from Table 1 in Ref. [3]: The center is on glide plane n, so these bold written positions have to be shifted by 3/4 3/4 0.

the coordinates $x(O_{H2})$ and $y(O_{H3})$ are erroneous in Table 1 of Ref. [3]. The $x(O_{H2})$ value is 0.05296 and not 0.5296, while the $y(O_{H3})$ value is 0.8201 and not 0.08201. After these corrections, the two data sets appear identical in the accuracy of the measurements.

3.3. Structural transformation

The transition is of first order [2], although the change of symmetry (C2/c is a maximal nonisomorphic subgroup of R − 3c) would allow the phase transition to be of second order. The matrix elements of the transformation from R − 3c to C2/c are the following: $S_{11} = − 2$, $S_{12} = − 1$, $S_{13} = 0$, $S_{21} = 0$, $S_{22} = − 1$, $S_{23} = 0$, $S_{31} = 2/3$, $S_{32} = 1/3$, $S_{33} = 1/3$.

This matrix **S** is used for further calculating the structural parameters of the HT modification in the m subcell.

3.3.1. Lattice parameters

Variation of the lattice parameters a, b (m axis), c, β and the volume V as a function of temperature is reported in Fig. 3. They change discontinuously at T's = 35(1) °C. The cell edge b increases from 5.740 to 5.748 Å ($\Delta b/b = 0.2\%$) above T's, while the other parameters decrease: β change from 104.3° to 101.9° ($\Delta\beta/\beta = − 2\%$), c from 16.305 to 15.98 Å ($\Delta c/c = − 2\%$), V from 904 to 895 Å^3 ($\Delta V/V = − 1\%$) and a from 9.970 to 9.555 Å ($\Delta a/a = − 0.2\%$). Upon cooling, the transition back to the m phase does not present hysteresis phenomena within the accuracy of the temperature measurement. Nevertheless, an hysteresis of the order of one degree was observed by polarized light microscopy [2].

3.3.2. Atomic displacements

The transformation matrix **S** from the rh → m system was applied to the coordinates (inverted matrix applied in fact to the coordinates of Ca, Al, Cl and O_W atoms). The results are reported in Table 4. It appears that the reversible transition rh↔m leads mainly to a displacement of 0.45 Å of the chloride anions along $[010]_h$ and to a displacement of 0.25 Å of the water molecules along $[210]_h$. The movement of the interlayer formed by chloride anions is represented on Fig. 4. The main layers can be consider as fixed. The transition leads to a glide of the planes formed by Cl^- anions along $[010]_h$. This direction becomes the direction of the m b-axis. The shifts of the
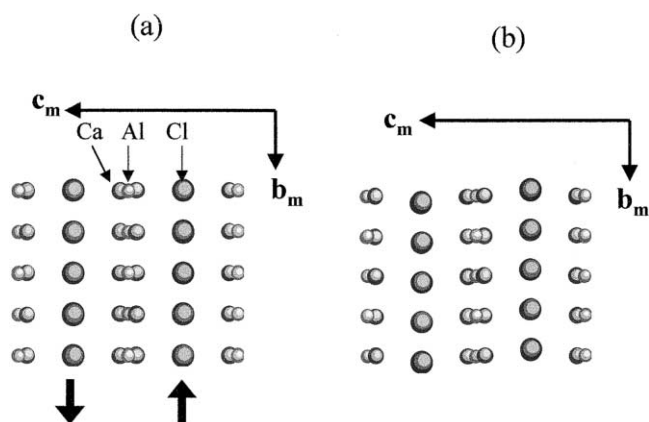

Fig. 3. Partial structure of $[Ca_2Al(OH)_6]^+[2H_2O, Cl^-]$ of the HT (a) and LT (b) modifications both orientated along the axis a_m of the m cell. The arrow in (a) allows visualizing the relative movement or glide of the sheets along the b_m axis (which is also the b_h direction) leading to the monoclinically distorted structure in (b).

Table 4
Coordinates of the heavy atoms above and below the transition (T's = 35 °C) in the C2/c m cell

Atom	$T = 40$ °C			$T = 20$ °C		
	X	Y	Z	X	Y	Z
Al	3/4	3/4	0.0 (−)	3/4	3/4	0.0 (−)
Ca	0.0957 (−)	3/4	0.0372 (7)	0.0984 (4)	0.7471 (7)	0.0377 (2)
Cl	0	1/4	1/4	0	0.3283 (11)	1/4
O_W	0.1485 (2)	0.75 (−)	0.1965 (2)	0.1729 (10)	0.7453 (23)	0.1993 (6)

interlayer species, Cl^- and water molecules, are also represented on Fig. 5. The positions of hydrogen atoms of the water molecules, not refined with our powder data, are taken from earlier single crystal data already discussed above [2,3].

The interatomic distances calculated with the IVTON program, a new version of the CSU program [15], are summarized in Table 5. Significant differences between the HT and LT modification occur mainly for the Cl–O distances and less with the Al–O distances in the octahedral environment of Al^{3+}. The Al(OH)$_6$ octahedra appear slightly compressed in the rh phase, in correlation with the decrease of the cell volume, compared to the same octahedra in the m phase (Al–O distances vary from 1.93 to 1.91 Å during the m → rh transition). The Ca–O distances, which are of course split in the m phase, do not change on the average during the structural transformation and remain approximately equal to 2.44 Å.

3.3.3. Origin of the transition

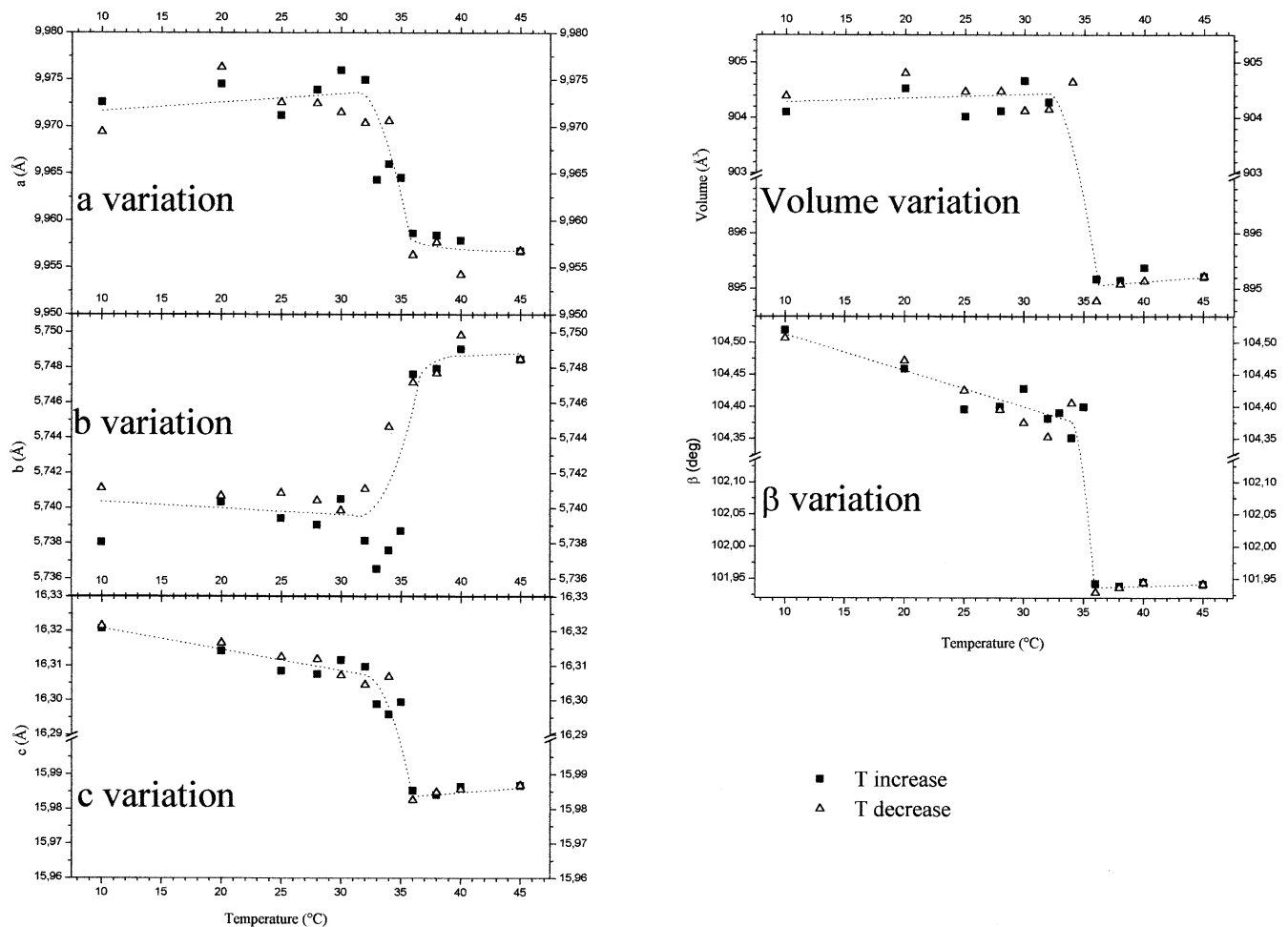In the HT modification (Fig. 5a), the Cl^- anions are for symmetry reasons perfectly in the center of a trigonal

Fig. 4. Lattice parameters of [Ca$_2$Al(OH)$_6$]$^+$ [2H$_2$O, Cl$^-$] as a function of temperature. Above the phase transition temperature, the rh cell is described with the m subcell: $a_m = -2a_h - b_h$; $b_m = -b_h$, $c_m = 2/3a_h + 1/3b_h + 1/3c_h$.
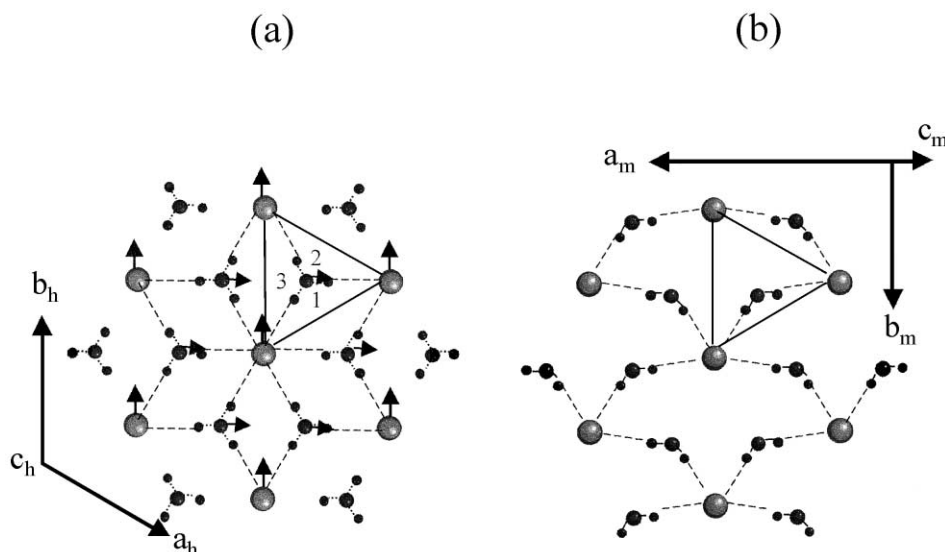
Fig. 5. Interlayer structure of $[Ca_2Al(OH)_6]^+[2H_2O, Cl^-]$ in the rh {represented by a projection along c_h axis} (a) and m {represented by a projection on (a_m, b_m) plane} (b) modifications.

antiprism formed by six water molecules, with six equivalent distances of 3.421 Å as indicated in Table 5. Each Cl^- is linked by hydrogen bonds (dashed lines on the drawing) to four H-atoms belonging to the interlayer water molecules. In the rh modification, due to the significant thermal displacements (see Table 2) of the interlayer species, the water molecules have orientational disorder as indicated by the partial occupancy of 2/3 for the H_W atoms. This means that each water molecule at the center of a regular triangle formed by three Cl atoms have three possible orientations noted 1−3 on the drawing. This is in agreement with molecular dynamic simulation (MDS) recently realized on Friedel's salt [17]. The authors concluded that the orientational disorder of the water molecules is dynamical.

At this step of the discussion, it is worthwhile to emphasize the main results of this work and to compare them with our own results. The starting parameters used for MDS were deduced from the coordinates of the m modification given by Terzis. The simulated lattice parameters they obtained, although not far from those given by Terzis, are closer to the parameters of the rh modification we determined later [2] than those of the m modification. It is especially true for the β angle, for which the simulated value is 101.84° at 0 °C, i.e. the same value we found for β of the HT rh modification described in the m subcell. However, this agreement is not surprising. As was pointed out by the authors, during the simulation, the hydrogen bonds virtually keep the «chloride anions in a static position». As we have shown in this paper, the structural phase transition leads to a relative shift of the chloride anions (see Table 3). Thus, we think that these molecular dynamic calculations [17] better simulate the rh phase than the m phase.

Kirkpatrick et al. [18] pointed out a hypothetical structural transformation at 6 °C from C2/c to P2/c from ^{35}Cl

NMR results. However, these authors did not have any knowledge of the structural phase transition partially described earlier [2]. The structural transition seen at 6 °C probably corresponds to the transition C2/c → R − 3c detailed here but at a lower temperature. It is worth pointing out that their compound contained a small proportion of carbonate as indicated by the chemical composition analysis $Ca_{1.96}Al_{1.04}(OH)_6Cl_{0.76}(CO_3)_{0.14}\cdot2H_2O$ they gave [18]. XRD single crystal results, not yet published, indicate that the carbonate contaminated Friedel's salt $[Ca_2Al(OH)_6]^+[Cl_{0.5}(CO_3)_{0.25}\cdot2H_2O]^-$ is rh at room temperature and does not transform down to liquid nitrogen temperature (77 K). Thus, we think that the temperature shift is undoubtedly due to contamination of the Friedel's salt by carbonates. It would be interesting to study the structural

Table 5
Selected interatomic distances (Å) Ca−O, Al−O of Friedel's salt of the HT and LT modifications

40 °C (R − 3c)			20 °C (C2/c)		
Al	$6O_H$	1.911 (6)	Al	$2O_{H2}$	1.939 (4)
				$2O_{H1}$	1.942 (11)
				$2O_{H3}$	1.956 (10)
Ca	$3O_H$	2.413 (4)	Ca	O_{H1}	2.362 (10)
				O_{H3}	2.366 (14)
				O_{H2}	2.379 (14)
	$3O_H$	2.431 (5)		O_{H2}	2.475 (10)
				O_{H1}	2.479 (9)
				O_{H3}	2.487 (10)
	O_W	2.517 (10)		O_W	2.547 (10)
Cl	$6O_W$	3.421 (2)	Cl	$2O_W$	3.173 (13)
				$2O_W$	3.190 (10)
				$2O_W$	3.940 (13)
	$6O_H$	3.448 (4)		$2O_{H2}$	3.224 (6)
				$2O_{H1}$	3.506 (11)
				$2O_{H3}$	3.651 (5)

transition in the solid solution $[Ca_2Al(OH)_6]^+[Cl_{1-x}(CO_2)_{x/2} \cdot 2H_2O]^-$.

The shifts of the interlayer species during the transition have been represented by arrows on Fig. 5a. These shifts lead to the m form represented on Fig. 5b. The water molecules approach along $[210]_h$ two chloride anions among the three forming a triangle. Consequently, the six Cl–O equivalent distances of 3.426 Å are split in four shorter distances (2×3.173 and 2×3.190 Å) and two longer ones of 3.940 Å. When the temperature is decreased, two stronger ClH bonds replace three weaker ones, which lead to a unique orientation per water molecule. In fact, the m distortion originates from the ordering of the hydrogen bond network, possible at a temperature lower than 35 °C, leading to a displacement of the interlayers formed by water molecule and Cl^- anions.

The transition enthalpy measured by DSC is 1.45(3) kcal/mol. Following our model, it corresponds, if we do not take into account the H-bonding between Cl and H of the hydroxyl groups, to the energy difference between two relatively strong hydrogen bonds ClH_W in the ordered m modification and the energy of three weaker hydrogen bonds in the disordered rh modification. This transition temperature is related to the hydration enthalpy of halogenide, $\Delta H_{hyd}(X^-)$, as indicated by a study not yet published, of the transition in the series X–AFm compounds where X can be Cl^-, Br^-, I^- or a mixture of these various anions.

4. Conclusion

This work, mainly based on synchrotron powder diffraction data, has brought out the main structural changes occurring in pure Friedel's salt during the m → rh transition at T's $= 35$ °C. The m distortion at a temperature lower than T's is due to an ordering of the water molecule orientation. The drastic changes in the hydrogen bond network lead to a decrease of the unit cell volume of 1% when heating from m → rh modification. It is thus significant to take account of this decrease of the volume occurring at ordinary temperature. It can be the cause of an increase in a open porosity in cements or concrete containing this phase in considerable quantity. It could be the case of concrete structures subjected to the action of chlorides contained for example in seawater. The mechanical properties of these concrete could be affected for it. On another side, the contamination by carbonates, coming from the atmospheric carbon dioxide, is beneficial since it blocks this structural transition.

Our LT data differ slightly from that given earlier by Terzis et al. [3].

The influence of the halide on the transition and the complete solid solution $[Ca_2Al(OH)_6]^+[Cl_{1-x}Br_x, 2H_2O]^-$ have been studied by X-ray synchrotron powder diffraction,

thermal analysis and polarized light microscopy. The manuscript is in preparation.

References

[1] P.M. Friedel, Sur un chloro-aluminate de calcium hydraté se maclant par compression, Bull. Soc. Fr. Minéral. 19 (1897) 122–136.

[2] G. Renaudin, F. Kubel, J.-P. Rivera, M. François, Structural phase transition and high temperature structure of Friedel's salt $3CaO \cdot Al_2O_3 \cdot CaCl_2 \cdot 10H_2O$, Cem. Concr. Res. 29 (1999) 1937–1942.

[3] A. Terzis, S. Filippakis, H.J. Kuzel, H. Burzlaff, The crystal structure of $Ca_2Al(OH)_6Cl \cdot 2H_2O$, Zeit Krist. 181 (1987) 29–34.

[4] J.-P. Rapin, N. Mohamed Noor, M. François, Double layered hydroxide $3CaO \cdot Al_2O_3 \cdot CaBr_2 \cdot 10H_2O$, Acta Crystallogr. C55 (1999) (part 8) http://www.iucr.ac.uk.

[5] J.-P. Rapin, A. Walcarius, G. Lefèvre, M. François, Double layered hydroxide $3CaO \cdot Al_2O3 \cdot CaI_2 \cdot 10H_2O$, Acta Crystallogr. C55 (1999) 1957–1959.

[6] R. Allmann, Refinement of the hybrid layer structure $[Ca_2Al(OH)_6]^+[1/2SO_4 \cdot 3H_2O]^-$, Neues Jahrb. Mineral., Monatsh. H3 (1977) 136–143.

[7] M. François, G. Renaudin, O. Evrard, A cementitious compound with composition $3CaO \cdot Al_2O_3 \cdot CaCO_3 \cdot 11H_2O$, Acta Crystallogr. C54 (1998) 1214–1217.

[8] G. Renaudin, M. François, O. Evrard, Order and disorder in the lamellar hydrated tetracalcium monocarboaluminate compound, Cem. Concr. Res. 29 (1999) 63–69.

[9] G. Renaudin, M. François, The lamellar double-hydroxide (LDH) compound with composition $3CaO \cdot Al_2O_3 \cdot Ca(NO_3) \cdot 10H_2O$, Acta Crystallogr. C55 (1999) 835–838.

[10] J. Nusovici, M.J. Winter, DIFFRAC-AT search, search/match using full trace as input, Adv. X-ray Anal. 37 (1994) 59–66.

[11] LURE W22 beamline:http://www.lure.u-psud.fr/Experiences/DCI/DW22.HTM.

[12] R. Argoud, J.J. Caponi, J. Appl. Crystallogr. 17 (1984) 420–425.

[13] A. Altomare, M.C. Burla, G. Cascarano, C. Giacovazzo, A. Guagliardi, A.G.G. Moliterni, G. Polidori, EXTRA: A program for extracting structure-factor amplitudes from powder diffraction data, J. Appl. Crystallogr. 28 (1995) 842–846.

[14] J. Rodriguez-Carvajal, M.T. Fernandez-Diaz, J.L. Martinez, J. Phys.: Condens. Matter 3 (1991) 3215–3234.

[15] I. Vickovic, CSU, a highly automatic and selective program for the calculation and presentation of geometrical parameters and their e.s.d.'s, J. Appl. Crystallogr. 21 (1988) 987–990.

[16] M. Evain, UFIT Program V1.3, Institut des Matériaux de Nantes, Nantes, France, 1992.

[17] A.G. Kalinichev, R.J. Kirkpatrick, R.T. Cygan, Molecular modeling of the structure and dynamics of the interlayer and surface species of mixed-metal layered hydroxides: Chloride and water in hydrocalumite (Friedel's salt), Am. Mineral. 85 (2000) 1046–1052.

[18] J. Kirkpatrick, Y. Ping, H. Xiaoqiang, K. Yeongkyoo, Interlayer structure, anion dynamics and phase transitions in mixed-metal layered hydroxides: Variable temperature ^{35}Cl NMR spectroscopy of hydrotalcite and Ca-aluminate hydrate (hydrocalumite), Am. Mineral. 84 (1999) 1186–1190.